Optically- and Thermally-Responsive Programmable Materials Based on Carbon Nanotube-Hydrogel Polymer Composites

Xiaobo Zhang,[†,‡,§] Cary L. Pint,[†,‡,§] Min Hyung Lee,[†,‡,§] Bryan Edward Schubert,[†] Arash Jamshidi,[†,‡] Kuniharu Takei,[†,‡,§] Hyunhyub Ko,[†,‡,§] Andrew Gillies,[†] Rizia Bardhan,[‖] Jeffrey J. Urban,[‖] Ming Wu,[†,‡] Ronald Fearing,[†] and Ali Javey*[,†,‡,§]

[†]Electrical Engineering and Computer Sciences and [‡]Berkeley Sensor and Actuator Center, University of California, Berkeley, California 94720, United States

[§]Materials Sciences Division and [‖]The Molecular Foundry, Lawrence Berkeley National Laboratory, Berkeley, California 94720, United States

ABSTRACT: A simple approach is described to fabricate reversible, thermally- and optically responsive actuators utilizing composites of poly(*N*-isopropylacrylamide) (pNIPAM) loaded with single-walled carbon nanotubes. With nanotube loading at concentrations of 0.75 mg/mL, we demonstrate up to 5 times enhancement to the thermal response time of the nanotube-pNIPAM hydrogel actuators caused by the enhanced mass transport of water molecules. Additionally, we demonstrate the ability to obtain ultrafast near-infrared optical response in nanotube-pNIPAM hydrogels under laser excitation enabled by the strong absorption properties of nanotubes. The work opens the framework to design complex and programmable self-folding materials, such as cubes and flowers, with advanced built-in features, including tunable response time as determined by the nanotube loading.

KEYWORDS: Poly(*N*-isopropylacrylamide), carbon nanotubes, programmable actuators, composites, responsive materials
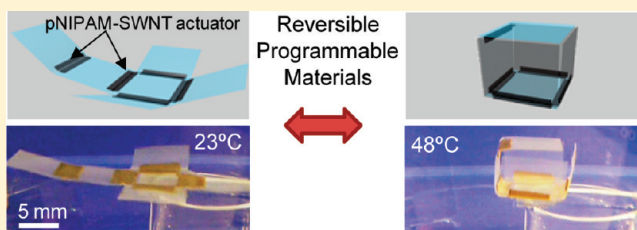
The conversion of external stimuli into mechanical motion capable of performing work is at the foundation of fields centered around the fabrication of microrobotics, artificial muscles, and advanced smart actuator systems for diverse applications.[1−5] Stimuli-responsive materials, such as shape memory alloys, dielectric polymers, electro-active polymers, and polymer hydrogels are examples of material frameworks that appeal to these emerging applications.[6−10] Specifically, poly(*N*-isopropylacrylamide) (pNIPAM) has emerged as one of the most extensively studied hydrogel systems for thermoresponsive polymer applications.[11] A key feature of this material system is a lower critical solution temperature (LCST) that occurs in the range of 32−33 °C, which is comparable to the temperature range which can be triggered by both physiological and environmental conditions.[11] Upon heating above the LCST, the hydrogel goes from a hydrophilic to hydrophobic state, resulting in a drastic change in the hydrogel volume by water expulsion.[11] In some cases, the hydrogels are loaded with functional nanomaterials that transform the response of radiation or chemical reactions to drive the LCST transition.[12−15] These features have made pNIPAM hydrogels excellent templates for a variety of biological and energy applications.[16]

Boasting extraordinary thermal, mechanical, and mass transport properties, while being compatible with aqueous solubilization techniques, carbon nanotubes[17,18] can be incorporated into pNIPAM hydrogels[19,20] with promise to yield significant improvements and new functionalities. In this study, we demonstrate single-walled carbon nanotube (SWNT)-pNIPAM composite hydrogels that exhibit up to 5 times enhancement in the thermal response time compared to pure pNIPAM hydrogels. Furthermore, the embedded SWNTs allow for efficient absorption of near-IR radiation, thereby resulting in ultrafast near-IR optically responsive hydrogels. Additionally, we demonstrate the arrangement of tunable SWNT-pNIPAM actuators into complex macroscale structures for the realization of programmable materials that reversibly change shape on user command.[21,22]

In order to fabricate SWNT-pNIPAM hydrogel strips, confinement channels with desired shapes and dimensions were made using Gel-Film (purchased from Gel-Pak, thickness, 342 μm) on a glass substrate (Figure 1a). The Gel-Pak film contains a polyester film with adhesive coating on one side and a Gel material on the other side. The adhesive layer firmly attaches the film onto the glass substrate while NIPAM curing is performed on the Gel surface. An aqueous solution of NIPAM monomer, *N,N'*-methylene-bis-acrylamide (bis-AMD, photo initiator), 2,2'-diethoxyacetophenone (DEAP, cross-linker), and sodium deoxycholate (DOC, surfactant)-SWNT (concentration, 0−1.0 mg/mL) was poured into the channels and covered with a glass slide to insulate the solution from air. Polymerization was performed by UV light irradiation (365 nm, 18.4W) for two hours, resulting in SWNT-pNIPAM composite strips loaded with varying amount of SWNTs (Figure 1b).
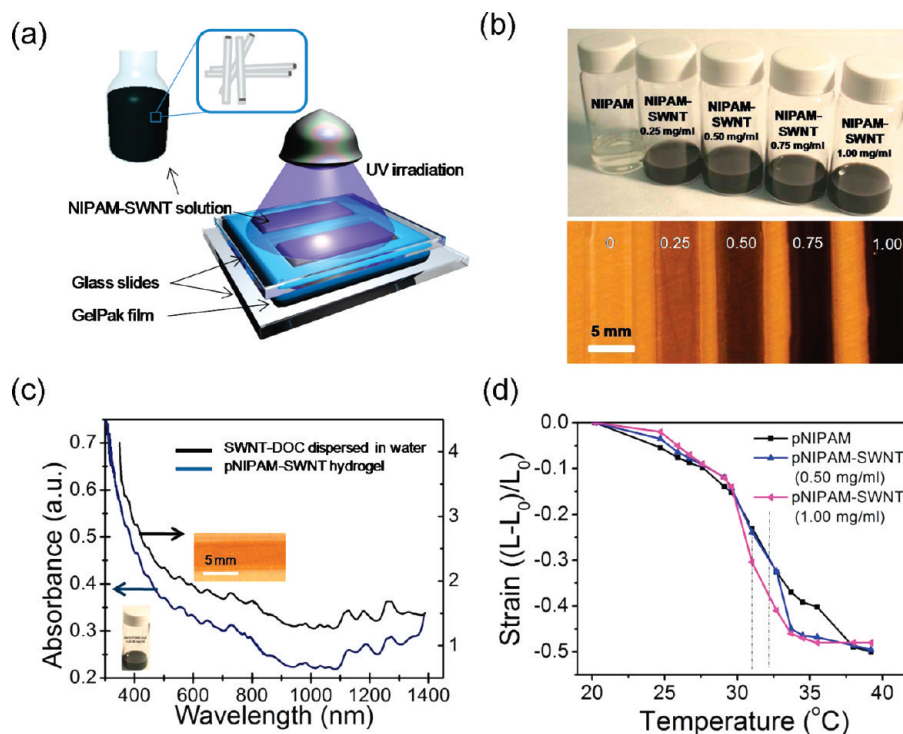
Figure 1. SWNT-pNIPAM hydrogel fabrication and characterization. (a) Polymerization scheme for making SWNT-pNIPAM hydrogels using Gel-Pak confinement channels and UV curing. (b) Polymer strips with different SWNT concentrations made using the method shown in panel a. (c) UV−vis-nIR absorption spectra of aqueous SWNT-DOC solution (blue) and a SWNT-pNIPAM hydrogel strip (SWNT concentration, 0.5 mg/mL) after polymerization (black). (d) LCST characterization for the polymer strips with different SWNT concentrations.

An important consideration for high quality composites is the uniform SWNT dispersion in the p-NIPAM hydrogels. Here, we utilized an aqueous 2 wt % DOC solution as the surfactant to disperse HiPCO SWNTs (Unidym, average diameter around 1.0 nm) at concentrations of up to 1 mg/mL using an ultrasonic bath. The SWNT dispersion is performed by intense sonication for at least one hour. At this stage, we except majority of the SWNTs to be open ended. Compared to other known surfactants for SWNT dispersion, such as sodium dodecyl sulfate or sodium dodecylbenzene sulfonate, we found DOC to be more stable in NIPAM monomer solutions.[23] The DOC-SWNTs and NIPAM monomer solutions formed homogeneous mixtures that exhibited stability to SWNT flocculation for several weeks. The dispersion quality was characterized by absorption studies. Figure 1c shows the UV−vis-nIR absorption spectra of as-prepared SWNT-DOC solution and the SWNT-pNIPAM hydrogel after UV polymerization. Both samples exhibit near identical absorption spectra with the absorption bands for the semiconductor ($E_{11} \sim 870-1300$ nm and $E_{22} \sim 500-800$ nm) and metallic SWNTs ($E_{11} \sim 400-600$ nm) clearly distinguished, confirming the good dispersion at the concentrations studied here.[24,25]

To measure the LCST of the SWNT-pNIPAM hydrogels, polymer strips (50 mm × 5 mm × 0.34 mm) with four different nanotube concentrations (0, 0.25, 0.50, and 1.0 mg/mL) were made using the aforementioned method as shown in Figure 1a. These strips were then immersed in a temperature-controlled water bath and the length of the polymer strips was measured as a function of temperature. To ensure the hydrogel is close to equilibrium, the temperature was increased in increments of 1 °C, and the measurements were taken 40 min after the water

had reached the target temperature. As shown in Figure 1d, the LCST temperature does not appear to be significantly influenced by the incorporation of SWNTs into the polymer hydrogels. Upon close inspection, it seems that the polymer strips with 1 mg/mL SWNTs have a slight depression of the LCST 1−2 °C compared to the pure pNIPAM strips, but this depression is comparable to the expected fitting error from the measurements. Nonetheless, the fact that the LCST in the SWNT-pNIPAM composites remains well-defined suggests that the incorporation of SWNTs into the polymer hydrogel does not influence the structure and the thermally induced phase transition of the polymer strips.

Next, we focus on the fabrication of thermally responsive actuator devices based on SWNT-pNIPAM composite hydrogels (Figure 2a) on low density polyethylene (LDPE, 50 μm in thickness, 16 mm × 8 mm) substrates. To accomplish this, we utilized a SWNT-pNIPAM/LDPE bilayer device scheme. In this device architecture, water loss in the SWNT-pNIPAM layer results in a mechanical strain that causes the actuation of the bilayer at predefined sites. Briefly, a parallel array of 10 hinge lines (depth, ∼25 μm; width, ∼30 μm; pitch, ∼80 μm) is patterned on the LDPE substrate using a computer-controlled laser writer to define the actuation sites. Next, an array of holes (diameter, 200 μm; pitch, 400 μm) are laser cut near the hinge lines in order to serve as anchoring sites for the subsequent deposition and polymerization of SWNT-pNIPAM (Figure 2a). A thin layer of SWNT-pNIPAM film (∼0.4 mm thick) was then directly formed onto the anchor holes by depositing the composite solution followed by UV polymerization. This forms a hinge that can fold up to 180° due to the abrupt strain change in the polymer hydrogel above the LCST. The folding dynamics of the hinges
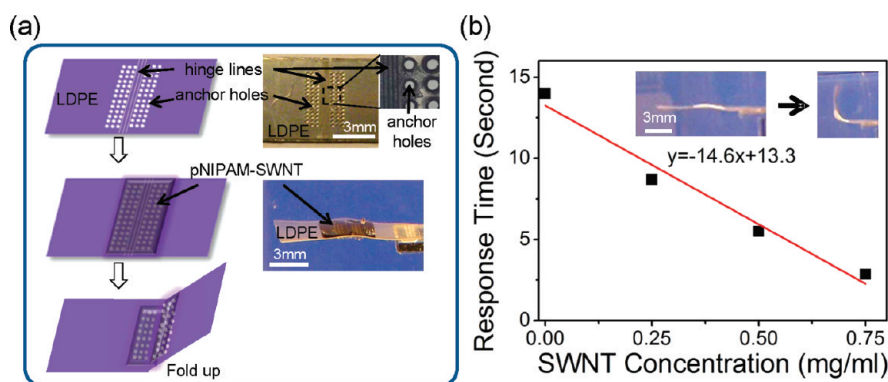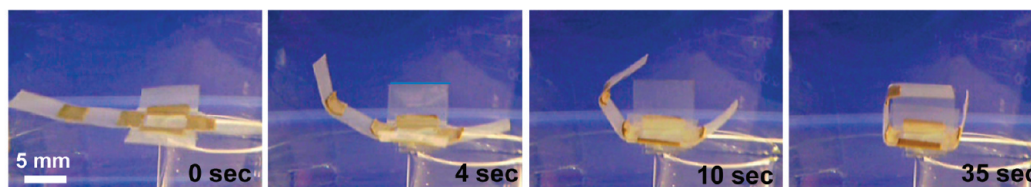
Figure 2. Fabrication scheme for making thermally responsive actuators and response time measurement. (a) Fabrication scheme for making SWNT-pNIPAM/LDPE bilayer actuators and the corresponding optical images. (b) Response time measurement by measuring the time for the actuator to reach 90° folding angle. The inset shows an optical image of a pNIPAM/LDPE actuator before (left) and right (after) folding.
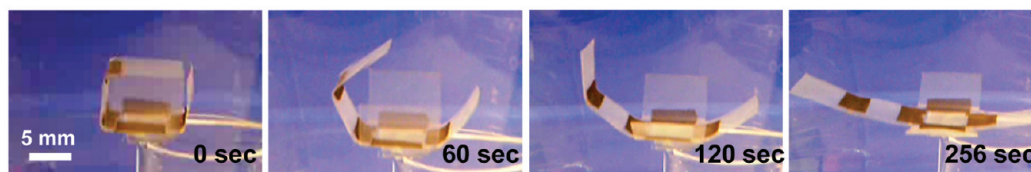

Figure 3. Programmable cubes — a folding cube based on thermal responsive actuators. (a) Fabrication scheme for folding cubes based on SWNT-pNIPAM/LDPE bilayer actuators. (b) Cube folding by thermal actuation in 48 °C water. (c) Cube reversibly unfolds by cooling down the water bath in which cube is immersed.
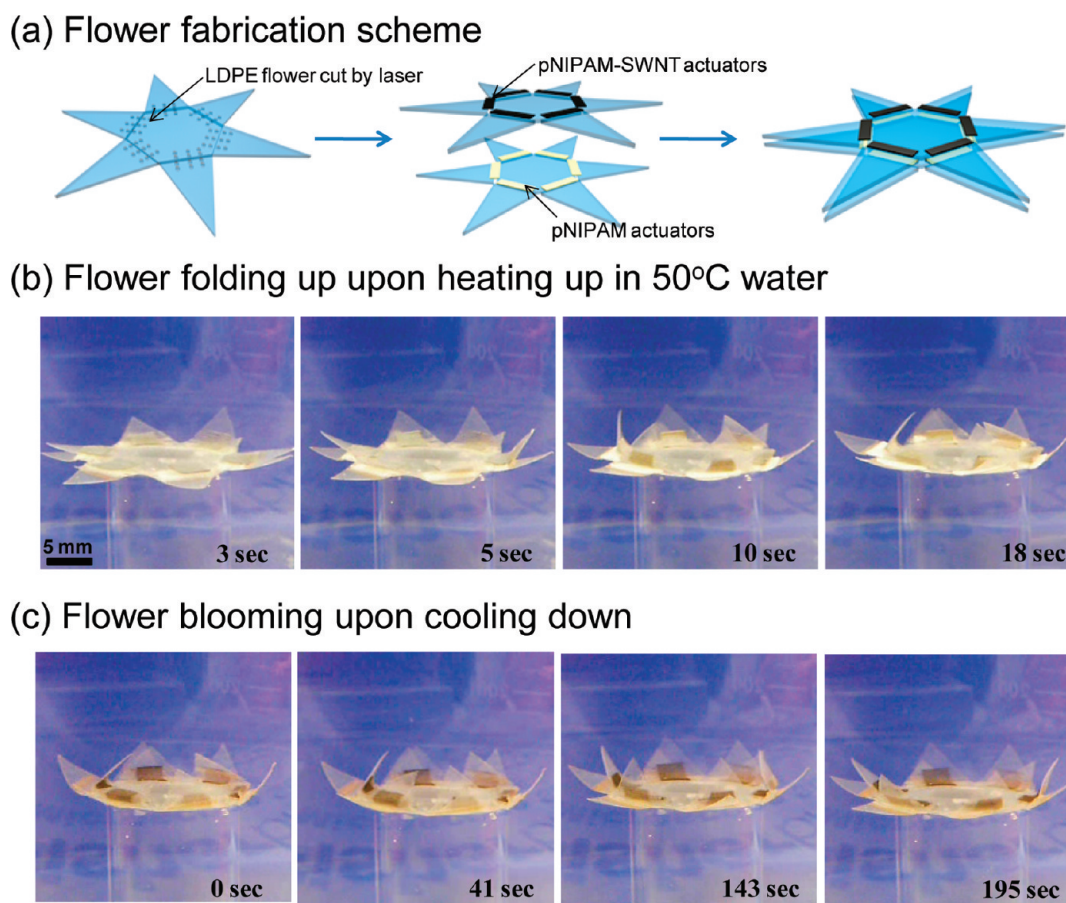
when transferred from a 23 to 55 °C water bath were characterized for SWNT concentrations of 0−0.75 mg/mL.

The response time, corresponding to the time required to reach a folding angle of 90° is shown in Figure 2b. The response time is found to linearly change with the SWNT content for the explored concentration range (0−0.75 mg/mL) with a slope of ∼−15 s/(mg/mL). Specifically, in the case of a hydrogel with 0.75 mg/mL of SWNTs, it takes ∼2.7 s for the hydrogel hinge to reach a 90° angle, compared to ∼14 s for the hydrogel without SWNTs. This leads to an overall maximum response time enhancement of ∼5 times through the incorporation of SWNTs into the polymer matrix.

Considering the mechanism by which the SWNTs enhance the response time, the result could be related to either one of two possible mechanisms: (i) enhancement of polymer composite thermal conductivity yielding faster heat transfer through the hydrogel, or (ii) enhancement of the mass (water) transport through the hydrogel due to the integration of SWNT fluidic channels in the hydrogel structure.[26,27] If we assume the thermal conductivity of pNIPAM hydrogel is equal to the thermal conductivity of water, simple heat transport modeling[28] reveals that the inner temperature of the hydrogel reaches the temperature of the hot water (55 °C) from an initial state of 25 °C in less than a second for the specific device dimensions explored here. Thereby, the response time is not limited by the heat transport since the time scale on which variations in thermal conductivity will influence the SWNT-pNIPAM response is significantly less than the actuator response time. Therefore, we propose the

(a) Flower fabrication scheme

(b) Flower folding up upon heating up in 50°C water

(c) Flower blooming upon cooling down

Figure 4. Programmable "flower' made by heterogeneous integration of pNIPAM and SWNT-pNIPAM bilayer actuators. (a) Fabrication scheme for making a programmable flower, consisting of two layers of actuators. (b) Flower folding (i.e., closes) when heated in a water bath to 50 °C. (c) Flower blooming by cooling down the water bath.
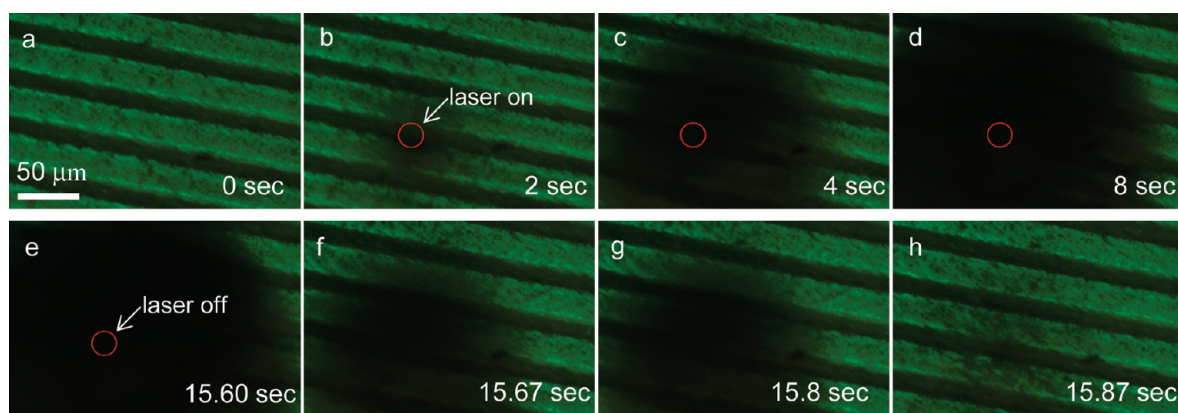
Figure 5. Near-IR optical response measurement for SWNT-pNIPAM hydrogels. (a) SWNT-pNIPAM/LDPE bilayer actuator (note: the background features are the hinge lines). (b—d) SWNT-pNIPAM hydrogel turns opaque (i.e., black) after illuminated by the near-IR laser beam from the top due to the shrinking of the SWNT-pNIPAM layer. (e—h) SWNT-pNIPAM hydrogel turns transparent after the laser beam is turned off which indicates the transition of the hydrogel back to a swelled state.

response time is instead limited by the mass transport of water and by the polymer chain reorganization (from hydrophilic to hydrophobic).[29] The addition of SWNTs into the pNIPAM hydrogel provides more porous (nano or microscale pores between pNIPAM and SWNTs) structures for enhanced water diffusion. In addition, previous reports have shown that carbon nanotubes can act as efficient channels for water flow driven by the osmotic pressure. Molecular dynamics simulation has shown that the flow rate can be as high as 5.8 molecules per nanosecond per nanotube and almost friction-less.[27] The diffusion coefficient of a hydrogel has been shown to be inversely proportional to the diffusion friction coefficient between the fluid and the network

which can be effectively reduced by adding of SWNT as shown here.[30]

We now demonstrate the ability to make "smart" or programmable devices based on the integration of SWNT-pNIPAM (0.5 mg/mL) hydrogel hinges arranged in complex assemblies. Shown in Figure 3a is the schematic of a cube fabricated using the concept of bilayer hinges (Figure 2a) made of SWNT-pNIPAM hydrogels. The cube template was fabricated on a laser patterned 50 μm LDPE film followed by the UV polymerization of SWNT-pNIPAM hydrogel patches on the hinges. When placed in warm water (48 °C), the strain induced by the shrinking hydrogel patches causes the cooperative folding of each hinge until the equilibrium shape of a cube is obtained. Figure 3a illustrates this process with a scheme, and Figure 3b,c shows that optical images of the cube folding and unfolding in a water bath after being heated to 48 °C, and subsequently cooled to 20 °C, respectively. In this case, the entire process of cube folding takes ~35 s, which is significantly faster than a similar device with only pNIPAM hydrogel hinges that would take up to ~150 s to perform the same function. The process is reversible and the closed cube can unfold completely when cooled down in water.

In addition to complex SWNT-pNIPAM hydrogel assemblies composed of only one type of hydrogel, we also demonstrate the ability to exploit the response time enhancement in the SWNT-pNIPAM hydrogels in the framework of a multilayer actuator architecture. Shown in Figure 4a is a design scheme for a multilayered patterned hinge resembling a flower, where the first layer of hinges are designed with a pNIPAM hydrogel (i.e., without SWNTs), whereas the second layer of hinges are composed of a SWNT-pNIPAM hydrogel that exhibits significantly enhanced response time. This allows the actuator device to exhibit an additional level of complexity that resembles the closing or blossoming of a real flower that has some leaves closing (blooming) earlier than others. Figure 4b shows a frame shot of this complex flower that is taken after the flower is placed in warm water (48 °C). In this case, even after 10 s of being immersed in the warm water, the hinges with the SWNT-pNIPAM have already reached a folding angle of over 90°, whereas the hinges with only pNIPAM hydrogels remain only slightly bent (<30°). Figure 4c shows the reverse process of the flower closing, depicting the process of a flower blooming with the inner "leaves" of the flower blooming faster than the outer leaves due to the enhanced response time of the SWNT-pNIPAM hydrogels compared to pNIPAM hydrogels used on the hinges. It should be noted that in all cases, the folding and unfolding processes were always found to be highly reversible with no noticeable degradation occurring in the thermally driven response for more than 20 cycles.

In addition, the use of SWNTs in the pNIPAM hydrogel templates yields an excellent route toward near-IR optically responsive hydrogel materials. pNIPAM is transparent in this wavelength range, and therefore unresponsive to near-IR irradiation. SWNTs have a well-defined near-IR optical absorption, specifically ideal for biocompatible devices such as drug delivery mediums or biological connector devices, since tissue and blood have a minimal near-IR absorptivity.[24,25] In order to demonstrate the optical response of SWNT −pNIPAM/LDPE bilayer actuators, we utilized a 785 nm laser (spot size ~20 μm) excitation with a power of ~30 mW. Transmission-mode optical images of a SWNT-pNIPAM hydrogel before, during, and after laser irradiation are captured using a CCD camera. As shown in Figure 5a, the hydrogel begins to develop a black (i.e., opaque) spot where the laser beam is positioned within 2 s of exposure due to the shrinking of the hydrogel by the local heat generated from near-IR absorption of SWNTs. This spot then spreads and reaches an equilibrium size after only ~8 s of exposure corresponding to the heat transport of the surroundings. Furthermore, after the laser is turned off, the pNIPAM hydrogel exhibits an ultrafast recovery to its original (transmissive) state within only 0.3 s. In contrast, control pNIPAM samples without SWNTs did not exhibit near-IR response (data not shown). The switching behavior of pNIPAM-SWNT composites was highly reversible after many cycles of switching; emphasizing that damage is not being incurred by the laser beam. This presents a new hydrogel medium with tremendous potential for ultrafast near-IR optical actuation relevant for numerous emerging biologically inspired applications.[31,32]

In summary, we have demonstrated a route to fabricating highly tunable, thermally and optically responsive actuator systems using SWNT-pNIPAM hydrogels. Utilizing an LDPE platform for making actuator hinges from the SWNT-pNIPAM hydrogels, we demonstrate that SWNTs enhance the response time of hydrogel actuation with the exact enhancement factor governed by the SWNT concentration. Utilizing this concept, we demonstrate complex assemblies of SWNT-pNIPAM hinge actuators, and specifically exploit the enhanced response time to add advanced function to these complex designs, such as a more accurate representation of a blooming flower. Finally, we demonstrate a well-defined, ultrafast response of the SWNT-pNIPAM hydrogel actuators to near-IR laser excitation, making this design viable for many optically triggered applications. We expect that the route to making SWNT-pNIPAM programmable actuators demonstrated here to be viable toward enabling a number of novel applications such as smart solar device tracking systems or tissue connectors for biological media.

■ AUTHOR INFORMATION

Corresponding Author
*E-mail: ajavey@eecs.berkeley.edu.

■ ACKNOWLEDGMENT

■ REFERENCES

(1) Brochu, P.; Pei, Q. *Macromol. Rapid Commun.* **2010**, *31*, 10–36.
(2) Ohm, C.; Brehmer, M.; Zentel, R. *Adv. Mater.* **2010**, *22*, 3366–3387.
(3) Mirfakhrai, T.; Madden, J. D. W.; Baughman, R. H. *Mater Today* **2007**, *10*, 30–38.
(4) Bassik, N.; Abebe, B. T.; Laflin, K. E.; Gracias, D. H. *Polymer* **2010**, *51*, 6093–6098.
(5) Leonga, T. G.; Randallb, C. L.; Bensona, B. R.; Bassika, N.; Sterna, G. M.; Gracias, D. H. *Proc. Natl. Acad. Sci. U.S.A.* **2009**, *106*, 703–708.
(6) Ratna, D.; Karger-Kocsis, J. *J. Mater. Sci.* **2008**, *43*, 254–269.
(7) Liu, F.; Urban, M. W. *Prog. Polym. Sci.* **2010**, *35*, 3–23.
(8) Lendlein, A.; Kelch, S. *Angew. Chem., Int. Ed.* **2002**, *41*, 2034–2057.

(9) Zhang, Q. M.; Li, H.; Poh, M.; Xia, F.; Cheng, Z. Y.; Xu, H.; Huang, C. *Nature* **2002**, *419*, 284–287.

(10) Yerushalmi, R.; Scherz, A.; van der Boom, M. E.; Kraatz, H. B. *J. Mater. Chem.* **2005**, *15*, 4480–4487.

(11) (a) Schild, H. G. *Prog. Polym. Sci.* **1992**, *17*, 163–249. (b) Liang, L.; Feng, X.; Liu, J.; Rieke, P. C.; Fryxell, G. E. *Macromolecules* **1998**, *31*, 7845–7850. (c) Rzaev, Z. M.O.; Dincer, S.; Piskin, E. *Prog. Polym. Sci.* **2007**, *32*, 534–595.

(12) Miyako, E.; Nagata, H.; Hirano, K.; Hirotsu, T. *Small* **2008**, *4*, 1711–1715.

(13) Hendrickson, G. R.; Smith, M. H.; South, A. B.; Lyon, L. A. *Adv. Funct. Mater.* **2010**, *20*, 1697–1712.

(14) Fujigaya, T.; Morimoto, T.; Niidome, Y.; Nakashima, N. *Adv. Mater.* **2008**, *20*, 3610–3614.

(15) Tokarev, I.; Minko, S. *Soft Matter* **2009**, *5*, 511–524.

(16) Kim, J.; Yoon, J.; Hayward, R. C. *Nat. Mater.* **2010**, *9*, 159–164.

(17) Javey, A. *ACS Nano* **2008**, *2*, 1329–1335.

(18) Dai, H. *Surf. Sci.* **2002**, *500*, 218–241.

(19) Fujigaya, T.; Morimoto, T.; Niidome, Y.; Nakashima, N. *Adv. Mater.* **2008**, *20*, 3610–3614.

(20) Wang, D.; Chen, L. *Nano Lett.* **2007**, *7*, 1480–1484.

(21) Maeda, S.; Hara, Y.; Sakai, T.; Yoshida, R.; Hashimoto, S. *Adv. Mater.* **2007**, *19*, 3480–3484.

(22) Cho, J. H.; Datta, D.; Park, S. Y.; Shenoy, V. B.; Gracias, D. H. *Nano Lett.* **2010**, *10*, 5098–5102.

(23) Kocharova, N.; Aaritalo, T.; Leiro, J.; Kankare, J.; Lukkari, J. *Langmuir* **2007**, *23*, 3363–3371.

(24) Weisman, R. B.; Smalley, R. E. *Science* **2002**, *297*, 593–596.

(25) Hauge, R. H.; Smalley, R. E.; Weisman, R. B. *Science* **2002**, *298*, 2361–2366.

(26) Kalra, A.; Garde, S.; Hummer, G. *Proc. Natl. Acad. Sci. U.S.A.* **2003**, *100*, 10175–10180.

(27) Joseph, S.; Aluru, N. R. *Nano Lett.* **2008**, *8*, 452–458.

(28) Widder, D. V. *The Heat Equation*; Academic Press, Inc.: New York, 1975.

(29) Okano, T.; Bae, Y. H.; Jacobs, H.; Kim, S. W. *J. Controlled Release* **1990**, *11*, 255–265.

(30) Li, Y.; Tanaka, T. *J. Chem. Phys.* **1990**, *92*, 1365–1371.

(31) Morimoto, M.; Irie, M. *J. Am. Chem. Soc.* **2010**, *132*, 14172–14178.

(32) Van Oosten, C. L.; Bastiaansen, C. W. M.; Broer, D. J. *Nat. Mater.* **2009**, *8*, 677–682.